Carbohydrate Polymers 92 (2013) 751–757

Contents lists available at SciVerse ScienceDirect

Carbohydrate Polymers

journal homepage: www.elsevier.com/locate/carbpol

Cellulose nanocrystals/polyurethane nanocomposites. Study from the viewpoint of microphase separated structure

L. Rueda[a], A. Saralegui[a], B. Fernández d'Arlas[a], Q. Zhou[b,c], L.A. Berglund[b,d], M.A. Corcuera[a], I. Mondragon[a], A. Eceiza[a,*]

[a] 'Materials + Technologies' Group, Department of Chemical and Environmental Engineering, Polytechnic School, University of the Basque Country, Pza. Europa 1, 20018 Donostia-San Sebastián, Spain
[b] Department of Fibre and Polymer Technology, Royal Institute of Technology, SE-100 44 Stockholm, Sweden
[c] School of Biotechnology, Royal Institute of Technology, AlbaNova University Centre, SE-106 91 Stockholm, Sweden
[d] Wallenberg Wood Science Center, Royal Institute of Technology, SE-100 44 Stockholm, Sweden

ARTICLE INFO

Article history:
Received 12 January 2012
Received in revised form
19 September 2012
Accepted 28 September 2012
Available online 9 October 2012

Keywords:
Cellulose nanocrystals
Polyurethane
Hard and soft segments
Atomic force microscopy
Crystallization

ABSTRACT

Cellulose nanocrystals (CNC) successfully obtained from microcrystalline cellulose (MCC) were dispersed in a thermoplastic polyurethane as matrix. Nanocomposites containing 1.5, 5, 10 and 30 wt% CNC were prepared by solvent casting procedure and properties of the resulting films were evaluated from the viewpoint of polyurethane microphase separated structure, soft and hard domains. CNC were effectively dispersed in the segmented thermoplastic elastomeric polyurethane (STPUE) matrix due to the favorable matrix–nanocrystals interactions through hydrogen bonding. Cellulose nanocrystals interacted with both soft and hard segments, enhancing stiffness and stability versus temperature of the nanocomposites. Thermal and mechanical properties of STPUE/CNC nanocomposites have been associated to the generated morphologies investigated by AFM images.

1. Introduction

The dispersion of reinforcing nanoparticles into a continuous polymer phase to form a nanocomposite has attracted a great deal of attention recently because it can provide significant improvements in thermal and mechanical properties at very low contents of the nanoreinforcement (Cao, Habibi, & Lucia, 2009). Cellulose constitutes the most abundant and renewable polymer resource available today and, as a chemical raw material, it has been used for a wide spectrum of products and materials in daily life (Qi, Cai, Zhang, & Kuga, 2009). Particularly, considerable interest has been recently focused on finding new material applications for cellulose. One of these efforts has been the development of cellulose nanocrystals. It is well known that cellulose fibers, when subjected to strong acid hydrolysis can be readily hydrolyzed to crystalline residues called cellulose nanocrystals (CNC) (Bondeson, Mathew, & Oksman, 2006; Dong, Revol, & Gray, 1998; Roman & Winter, 2004). The use of cellulose nanocrystals as a reinforcing material in composites is a relatively new field within nanotechnology that has generated considerable interest in the last decade, especially in bionanocomposite research, due to their low cost, high availability, renewability, nanoscale dimensions, easy for chemical modification, low density and good mechanical response (Habibi, Lucía, & Rojas, 2010).

However, there are several challenges in using cellulose nanocrystals combined with polymers which include the efficient separation of CNC from plant resources, compatibilization of the nanoreinforcements with the matrix and development of suitable methods for processing these nanocomposites (Siqueira, Bras, & Dufresne, 2009). Processing techniques have an important impact on the final properties of the composites. For this reason, several authors classified processing methods in ascending order of their reinforcement efficiency: extrusion < hot pressing < evaporation, associated to probable breakage and/or orientation of CNC during processing (Golapan Nai & Dufresne, 2003; Hajji, Cavaillé, Favier, Gauthier, & Virgier, 1996; Morin & Dufresne, 2002).

In this way, aqueous and solvent solution casting is the most common method of preparing cellulose nanocomposites (Goetz, Mathew, Oksman, Gatenholm, & Ragauskas, 2009). Due to the hydrophilic character of CNC, the simplest polymer systems that incorporate CNC are water-based. However, these systems suffer from limited utility and are only appropriate for water-soluble or dispersible polymers such latexes. On the other hand, the use of polar aprotic solvents, most commonly, N,N-dimethylformamide

* Corresponding author. Tel.: +34 943017185; fax: +34 943017200.
E-mail address: arantxa.eceiza@ehu.es (A. Eceiza).

0144-8617/$ – see front matter © 2012 Elsevier Ltd. All rights reserved.
http://dx.doi.org/10.1016/j.carbpol.2012.09.093

(DMF) has been explored to redisperse successfully freeze-dried CNC (Shanmuganathan, Capadona, Rowan, & Weder, 2010; Van den Berg, Capadona, & Weder, 2007). Azizi Samir, Alloin, Sanchez, El Kissi, and Dufresne (2004) showed via DMF suspension that it was possible to obtain composite materials which did not alter the formation of the percolating cellulosic network responsible for high mechanical properties.

In this study, polyurethane has been used as the matrix polymer. Polyurethanes are an interesting family of polymers which have been used for a variety of applications in a range of commodity products such as biomedical, coatings, foams, adhesives and composites (Seydibeyoglu & Oksman, 2008). Segmented thermoplastic elastomeric polyurethanes are versatile polymeric matrices typically constructed alternating soft (SS) and hard segments (HS). The thermodynamic incompatilibility between both segments drives the polymer system into a nano/microphase separation. The hard segments forming the crystalline phase offer stiffness to the resultant materials and the soft segments control low temperature properties. By simply adjusting the hard/soft segment ratio during the synthesis, functional polymers with different properties can be obtained (Hung & Hsu, 2009; Tien & Wei, 2006). In addition, the secondary structure in polyurethanes depends on the proximity zone interaction between HS and is mainly characterized by hydrogen bonding between adjacent urethane groups which causes relatively strong interactions, even when the hard segments are very short (Schauerte & Sundermann, 1994).

Therefore, to prepare high performance nanocomposite materials with a hydrophobic matrix and hydrophilic CNC fillers, the major issues to address are adequate dispersion and developing strong interfacial adhesion between the matrix and the reinforcement, essential to enhance composite properties. An effective way for this procedure is through hydrogen bonding taking advantage of the abundant hydroxyl groups (—OH) on the surface of CNC and carbonyl groups (—C═O) in polyurethane.

Moreover, the macroscopic behavior of CNC based nanocomposites depends on the specific behavior and volume fraction of each phase, the microstructure of the phases and also the interfacial properties, although the affinity between the matrix and the cellulosic materials can cause physical phenomenon as crystallization, directly linked to the aspect ratio of the nanocrystals (Azizi Samir, Alloin, & Dufresne, 2005). In general, mechanical properties of such materials are affected by parameters as the geometrical aspect ratio, the processing method and the matrix structure and the resulting competition interactions (matrix/filler and filler/filler interactions). Taking into account that the CNC aspect ratio and the processing method can be made common for nanocomposites, the evaluation of resulting interactions due to the affinity between matrix and CNC can determine differences in final materials properties.

In previous work, elastomeric nanocomposites were successfully prepared using microcrystalline cellulose (MCC) and CNC linked to polyurethane matrices by both covalent and hydrogen bonds (Pei, Malho, Ruokolainen, Zhou, & Berglund, 2011; Rueda et al., 2011; Wu, Henriksson, Liu, & Berglund, 2007). The aim of the work reported here was to study the effect of reinforcing a STPUE matrix with low/high contents of cellulose nanocrystals and also the effects of their dispersion can cause in thermal, morphological and mechanical properties of polyurethane nanocomposites through hydrogen bonding.

2. Materials and methods

2.1. Segmented thermoplastic elastomeric polyurethane

STPUE was synthesized by using a 2.332 g/mol block copolymer (polycaprolactone-b-polytetradydrofuran-b-polycaprolactone) diol (PCL-b-PTHF-b-PCL) from Sigma–Aldrich, 1,6-hexamethylene diisocyanate (HDI) kindly supplied by Bayer and 1,4-butanediol (1,4-BD) from Fluka, as chain extender. A two step polymerization was employed to synthesize a STPUE matrix containing 18 wt% of hard segment whose components were combined in the ratio 1:2:1. Firstly, the isocyanate-terminated prepolymer was prepared by reaction between the polydiol with the diisocyanate at 100 °C for 6 h in nitrogen atmosphere. Then, 1,4-BD was added at the same temperature during 5 min with vigorous stirring. Finally, the viscous mixture was transferred into a mold and kept in a vacuum oven at 100 °C for 24 h. The synthesis and characterization of this type of matrix was detailed elsewhere (Rueda-Larraz et al., 2009).

2.2. Isolation of cellulose nanocrystals

Deionized (DI) water/MCC-suspension was put in a temperature controller bath at 0 °C and stirred while concentrated sulfuric acid (95–97%) was added drop by drop until 64% acid concentration was reached. Then, the suspension was heated at 44 °C while stirred during 1 h and next was washed with DI water using repeated centrifugation cycles of 30 min at 9000 rpm (Specac, Meditronic BL-S) followed by resuspension of the solids in new DI water and mixed. The centrifugation step was stopped after the supernatant became turbid. The last washing step was conducted using dialysis against DI water to pH 5–6 and finally, samples were freeze-dried.

2.3. Nanocomposite preparation

Solutions of STPUE in DMF (25 mg/mL) were mixed with different amounts of CNC and sonicated in Vibracell 75043 from Bioblock Scientific at 0 °C for 2 h. Five composite films containing several CNC weight contents, 0, 1.5, 5, 10 and 30 wt% were prepared. Each STPUE and STPUE/CNC samples were solution cast onto teflon petri dishes and then they were subjected to a pressure-temperature cycle at 80 °C using a chemistry vacuum pumping unit (Vacuubrand PC 600 series) to obtain films with a thicknes of 0.1 mm. Polyurethane as matrix and nanocomposites were designated as STPUE, STPUE-1.5_{CNC}, STPUE-5_{CNC}, STPUE-10_{CNC} and STPUE-30_{CNC}.

3. Experimental

Differential scanning calorimetry (DSC) scans were recorded on a Mettler Toledo 822^e equipment. Samples were scanned from −60 °C to 150 °C at 10 °C min^{-1} under nitrogen atmosphere. Soft segment melting temperature (T_{mSS}) and hard segment melting temperature (T_{mHS}) were taken as the peak temperature of the corresponding melting endotherms. The melting enthalpy of soft and hard segments (ΔH_{mSS} and ΔH_{mHS}) was also measured from these endotherms. Besides, located between T_{mSS} and T_{mHS}, the transition temperature associated to amorphous hard segment chains (T_I) was also observed. Some authors referred this transition temperature as enthalpy relaxation endotherm for low hard segment content in polyurethanes (Chen, Shieh, & Chui, 1998; Cuve, Pascault, Boiteux, & Seytre, 1991; Eceiza et al., 2008; Koberstein, Galambos, & Leung, 1992; Saiani et al., 2007) and depending on the increase of HS content in polyurethanes, it could be associated to the glass transition of the hard domains (Azizi Samir et al., 2005; Pei et al., 2011).

Dynamic mechanical analysis (DMA) of the neat polyurethane and nanocomposites was carried out in tensile mode (DMA Q-800, TA Instruments). Measurements were performed at a constant frequency of 1 Hz, amplitude of 25 μm, a temperature range from −90 °C to 130 °C, a heating rate of 3 °C min^{-1} and a preload of 0.01 N. Samples were prepared by cutting strips with a width of 2.5 mm from the films. By this technique, the glass transition temperature of the soft segment (T_{gSS}) was defined as the temperature corresponding to the maximum value of the loss factor ($\tan\delta$).

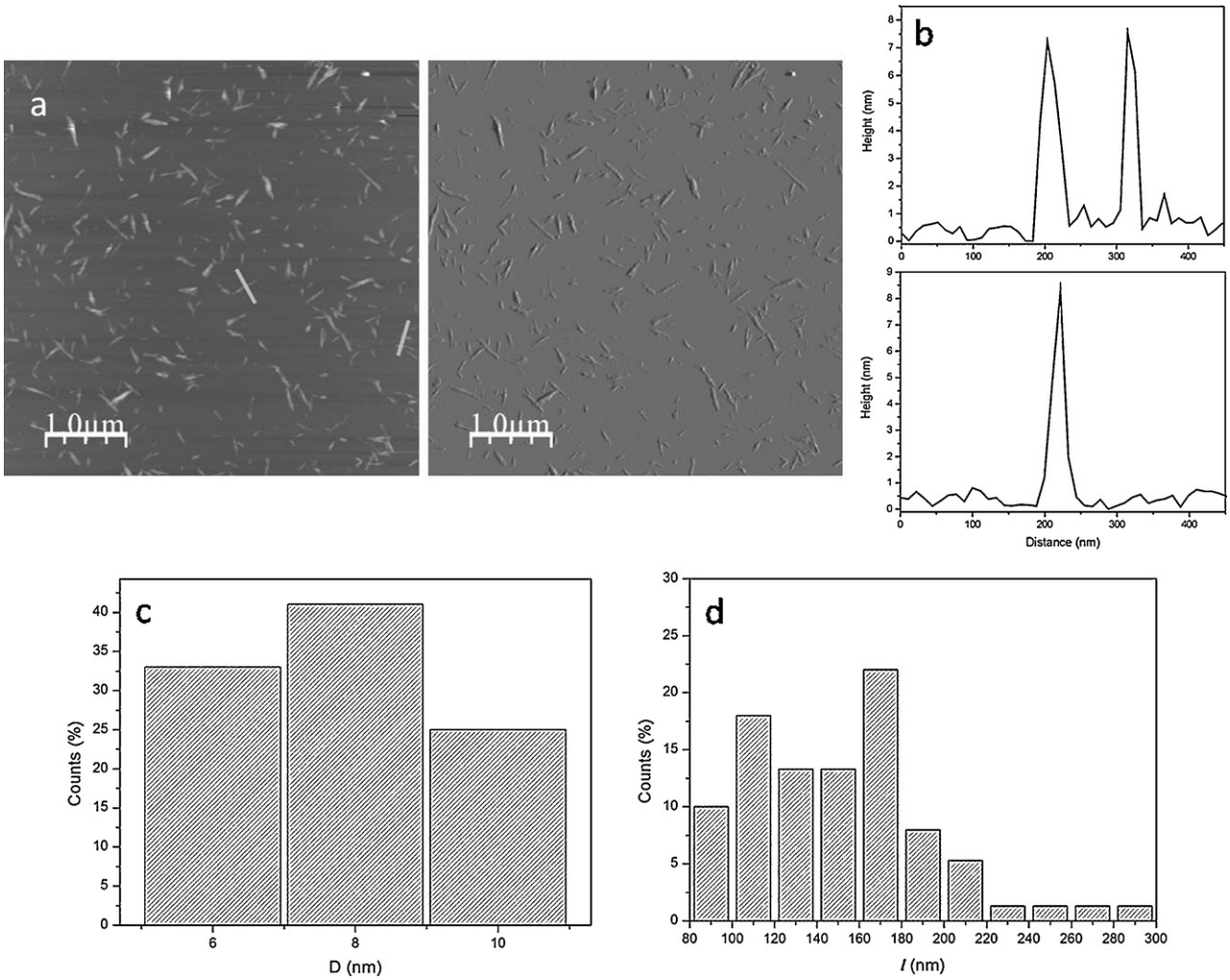

Fig. 1. Height (left) and phase (right) AFM images (a), height profiles (b) of CNC suspension in deionized water and diameter and length distributions (c and d) respectively, as obtained analyzing a population over 75 cellulose nanocrystals.

Tapping mode atomic force microscopy (TM-AFM) was used to visualize the images of CNC and STPUE nanocomposites on a Nanoscope IIIa, Multimode, Digital Instruments with an integrated force generated by cantilever/silicon probes, applying a resonance frequency of ~180 kHz. The cantilevers had a tip radius of 5–10 nm. CNC images were captured using RTESP probes with a cantilever spring constant in the range 20–80 N/m following the Beck-Candanedo, Roman, and Gray (2005) procedure to prepare the samples. The size distribution of cellulose nanocrystals was also determined by AFM taking into account 75 measurements of total CNC population in the height AFM image. Particle diameters were determined using the section analysis tool provided with the software WSxM 5.0 (Horcas et al., 2007). Since the nanocrystals are assumed to be cylindrical in shape, the height of the nanocrystals was taken to be equivalent to the diameter, to compensate for image widening due to the convolution of the tip and the particle. Length measurements were obtained from printouts of several height mode AFM images for each sample. Nanocomposite samples were prepared via spin-coating (Spincoater P6700) at 2000 rpm for 130 s and they were subjected to annealing in an oven at 100 °C for 12 h. Solvent cast nanocomposite films sections were also imaged and were prepared using a Leica EM FC6 cryo-ultramicrotome equipped with a diamond knife and operated at −120 °C.

Samples for mechanical behavior were prepared by cutting strips from nanocomposite films with a thickness of 0.1 mm obtained by solvent casting in according to ASTM D 1708-93. MTS equipment with a load cell of 250 N was used to measure tensile modulus (E), tensile strength at maximum elongation (σ), yield strength at 50% offset (σ_{50}) and strain at break (ε_b). Tests were performed at 100 mm/min and results were averaged out from five test specimen data.

4. Results and discussion

The morphology of the CNC obtained by acid hydrolysis is shown in Fig. 1. The white lines in the height or topography AFM image (Fig. 1a, left) are associated to height profiles of CNC (Fig. 1b), which corresponds to the diameter as explained before. Additionally, Fig. 1c and d represents the diameters and length distributions, respectively, as obtained analyzing a population over 75 cellulose nanocrystals. Acid hydrolysis of MCC led to rod-like CNC with an average diameter of 8 ± 0.7 nm and length of about 137 ± 35 nm. These values are in agreement with CNC aspect ratio from similar sources reported in literature (Habibi et al., 2010), corresponding to an average aspect ratio of 17 ± 6, approximately.

Thermal properties of cellulose nanocrystals reinforced polyurethanes were determined from DSC thermograms. Thermal transitions related to the microphase separation of soft segments from hard segments are shown in Fig. 2 and collected in Table 1. Polyurethane matrix and their nanocomposites showed the same temperature transitions and endotherms. On this way, the melting

Table 1
DSC data recorded for neat polyurethane and their nanocomposites prepared by the incorporation of CNC. Soft segment melting temperature, soft segment melting enthalpy, hard segment enthalpy relaxation endotherm, hard segment melting temperature and hard segment melting enthalpy.

Sample	T_{mSS} (°C)	ΔH_{mSS} (J/g)	T_I (°C)	T_{mHS} (°C)	ΔH_{mHS} (J/g)
STPUE	−0.5	9.37	55	107	0.4
STPUE-1.5$_{CNC}$	−1	12.9	50	107	0.6
STPUE-5$_{CNC}$	0.5	14.5	53	106	1.6
STPUE-10$_{CNC}$	4.5	8.63	55	101	2.6
STPUE-30$_{CNC}$	−1	10.0	53	102	1.7

temperature endotherm and melting enthalpies associated to the soft segment and hard segments were clearly seen. In addition, at T_I region (50–55 °C), a broader endotherm was also found when CNC content increased, which can be associated to the amorphous hard segment interactions as well as to hydrogen bonding of amorphous hard segment chains with CNC. As can be observed in Table 1, whereas T_{mSS} was not drastically influenced by the incorporation of CNC, ΔH_{mSS} increased significantly in polyurethane nanocomposites with lower CNC content (from 1.5 and 5 wt%), which can be ascribed to strong interactions between SS chains and CNC. However, T_{mHS} decreased in STPUE-10$_{CNC}$ and STPUE-30$_{CNC}$ where CNC could act as nucleating agent. On the other hand, all nanocomposites showed an increase in ΔH_{mHS}, which can be related to the interactions of CNC with hard segment chains in this phase as well. These results indicate that CNC favored crystallization in both SS and HS segments which may stem from well dispersed nanoreinforcements that maximize matrix–cellulose interactions (Auad, Contos, Nutt, Aranguren, & Marcovich, 2008) through hydrogen bonding, taking advantage of the abundant hydroxyl groups (—OH) on the surface of CNC and carbonyl groups (—C=O) in both polyurethane segments.

Great interest has been focused on investigating the use of CNC as a reinforcing phase in a polymeric matrix to evaluate the microstructure-property relationships of the resulting nanocomposites (Capadona et al., 2009; Holt, Stoyanov, Pelan, & Paunov, 2010) These investigations can be performed by DMA, which allows the determination of the mechanical behavior of materials in a broad temperature/frequency range as a function of the nanocomposite microstructure.

The storage modulus (E') and loss factor as a function of temperature of the cast films of neat polyurethane and nanocomposites are shown in Fig. 3. In the glassy state at very low temperature, E' was significantly higher when CNC content increased in the nanocomposite. In this way, STPUE-30$_{CNC}$ showed an E' increase of 350% respect to the value of polyurethane matrix. At low temperature, polyurethane properties are governed by the soft phase. In this region, the storage modulus slightly decreased with temperature but remained roughly constant due to the molecular motions were largely restricted to vibration and short-range rotation. As the temperature increased, the storage modulus showed a significant decrease. This temperature range, between −70 and −50 °C, corresponds to the main relaxation process of the soft phase in polyurethanes and polyurethane nanocomposites, associated to the glass transition temperature. The loss factor showed a maximum at −57 °C associated with this transition that remained nearly at the same position as CNC content was incorporated to the nanocomposite. However, it is possible to observe a broadening in the loss factor when CNC content increased, which can be related to the molecular mobility of amorphous macromolecular chains, slightly affected by the presence of CNC. Some authors found that cellulose nanocrystals cause reduced molecular mobility of the matrix close to the fiber (Berglund, 2005; Chazeau, Paillet, & Cavaille, 1999; Dufresne, 2000) This effect is also evidenced by a sharp decrease in tan δ peak area and height and indicative that the fraction of polyurethane matrix molecules participating in the T_g decreases as the cellulose content increases. Above this temperature, the value of E' kept decreasing upon temperature showing two plateau regions. In the first plateau, extended from −50 °C to 15 °C, nanocomposites showed an improvement in E' related to the reinforcing effect of the CNC. At higher temperature, the storage modulus showed a new decrease, corresponding to the melting range of the soft segment. Above this temperature, in the second plateau region, neat polyurethane showed a small plateau followed by an abrupt drop which can be related to some relaxation effects of polymer chains in the hard segment phase corresponding to the enthalpy relaxation endotherm of the hard segment and hard segment structures disruption. On the other hand, nanocomposites showed an improvement in storage modulus because of

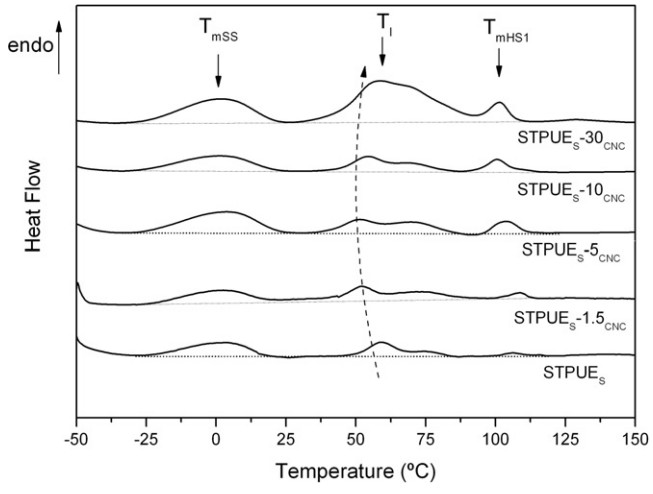

Fig. 2. DSC thermograms for STPUE, STPUE-1.5$_{CNC}$, STPUE-5$_{CNC}$, STPUE-10$_{CNC}$ and STPUE-30$_{CNC}$.

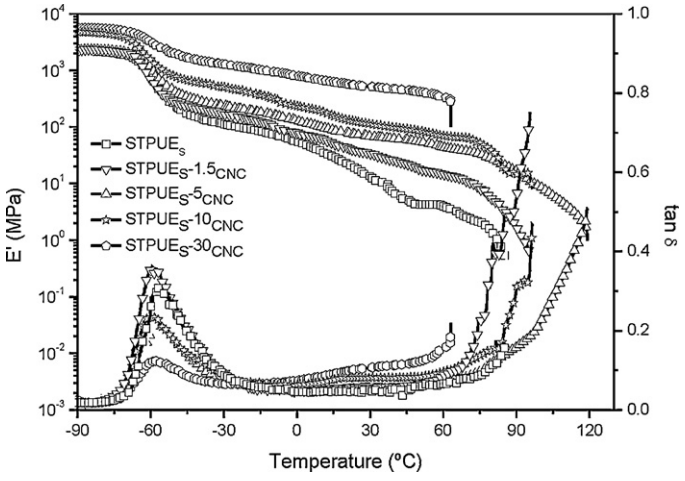

Fig. 3. Storage modulus and loss factor versus temperature for polyurethane and polyurethane nanocomposites: STPUE (□), STPUE-1.5$_{CNC}$ (▽) STPUE-5$_{CNC}$ (△), STPUE-10$_{CNC}$ (☆) and STPUE-30$_{CNC}$ (⏢).

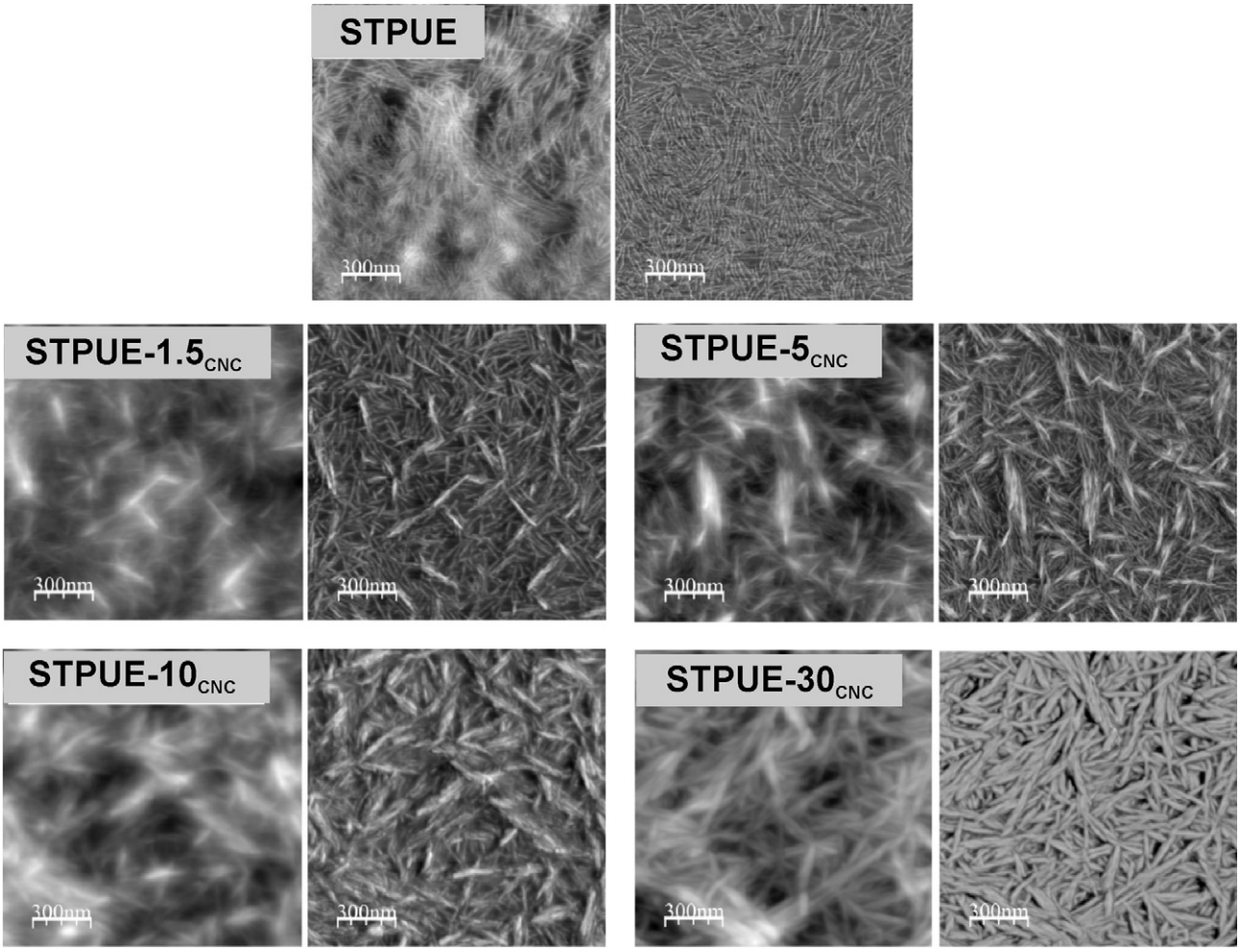

Fig. 4. AFM height (left) and phase (right) images of annealed polyurethane and polyurethane nanocomposites at 100 °C for 12 h.

effective CNC dispersion, and due to the filler–matrix interactions, which enhances hard segment crystallinity, decreasing molecular mobility and promoting rigidity. In this way, STPUE-5_{CNC} showed an increase in stability with temperature in the second plateau region which was extended until 120 °C and could be ascribed to filler–matrix interactions through hydrogen bonding and also due to hard segment crystalline enhancement, as observed by DSC. However, it is worth nothing that for high nanocrystals content, 30 wt%, the behavior was different as the stability upon temperature decreased. It could be due to the lack in cohesion between polyurethane amorphous and crystalline hard domains related to the high CNC content, which played the role of both filler particles and physical cross-links for the system. Parameters which can directly be affected with the CNC network formation or interfere with it are the polyurethane microstructure and the matrix–nanoreinforcement interaction (Ling, Huang, Chang, Anderson, & Yu, 2011) Besides, in semicrystalline matrices, the crystallization induced by CNC can provoke the breakdown of the CNC network. As can be observed in DMA results, E' started to dramatically decrease from T_I confirming that CNC network was not formed in these polyurethane nanocomposites.

Atomic force microscopy has proven to be an important tool to elucidate the microphase separated structure at nanoscale levels. The morphology of the annealed and cryo-ultramicrotomed sections of STPUE and STPUE/CNC nanocomposites was imaged using tapping-mode AFM. Figs. 4 and 5 show phase and height features, respectively. In general, in the phase image (right), lighter regions correspond to hard phase material (crystalline regions in polyurethane matrix or HS) and darker regions are associated to soft phase material (polyol or SS). AFM images for STPUE revealed very small size of hard segment domains due to the small quantity of hard segment involved. In addition, Fig. 4 shows an effective CNC dispersion in polyurethane matrix solution when spin coated films are obtained indicative of interactions between them. On the other hand, Fig. 5 displayed AFM images of the final nanocomposites where a relatively uniform CNC dispersion in polyurethane matrix is observed using solvent casting as procedure.

The characteristic values derived from stress–strain curves are presented in Table 2. The tensile curve of neat polyurethane can be analyzed in three distinct zones taking into account the SS and HS microdomains (Liff, Kumar, & Mckinley, 2007) The first region, where the stress increases linearly with the strain, is related to the elastic deformation governed by polyurethane crystallinity, HS content and ordering (Wang & Cooper, 1983) Yield corresponds to break-up of an interconnected hard-domain network

Table 2
Mechanical properties of STPUE and nanocomposites. Young's modulus, yield strength at 50% offset, tensile strength, and strain at break.

Sample	E (MPa)	σ_{50} (MPa)	σ (MPa)	ε_b (%)
STPUE	14.2 ± 0.4	1.9 ± 0.2	7.4 ± 0.7	1529 ± 257
STPUE-1.5_{CNC}	15.4 ± 3.8	2.0 ± 0.2	9.4 ± 1.3	1587 ± 26
STPUE-5_{CNC}	28.5 ± 6.0	2.4 ± 0.1	5.3 ± 0.4	776 ± 60
STPUE-10_{CNC}	41.4 ± 9.5	3.7 ± 0.2	6.9 ± 0.2	536 ± 115
STPUE-30_{CNC}	109 ± 9.4	5.3 ± 0.2	6.2 ± 0.3	195 ± 34

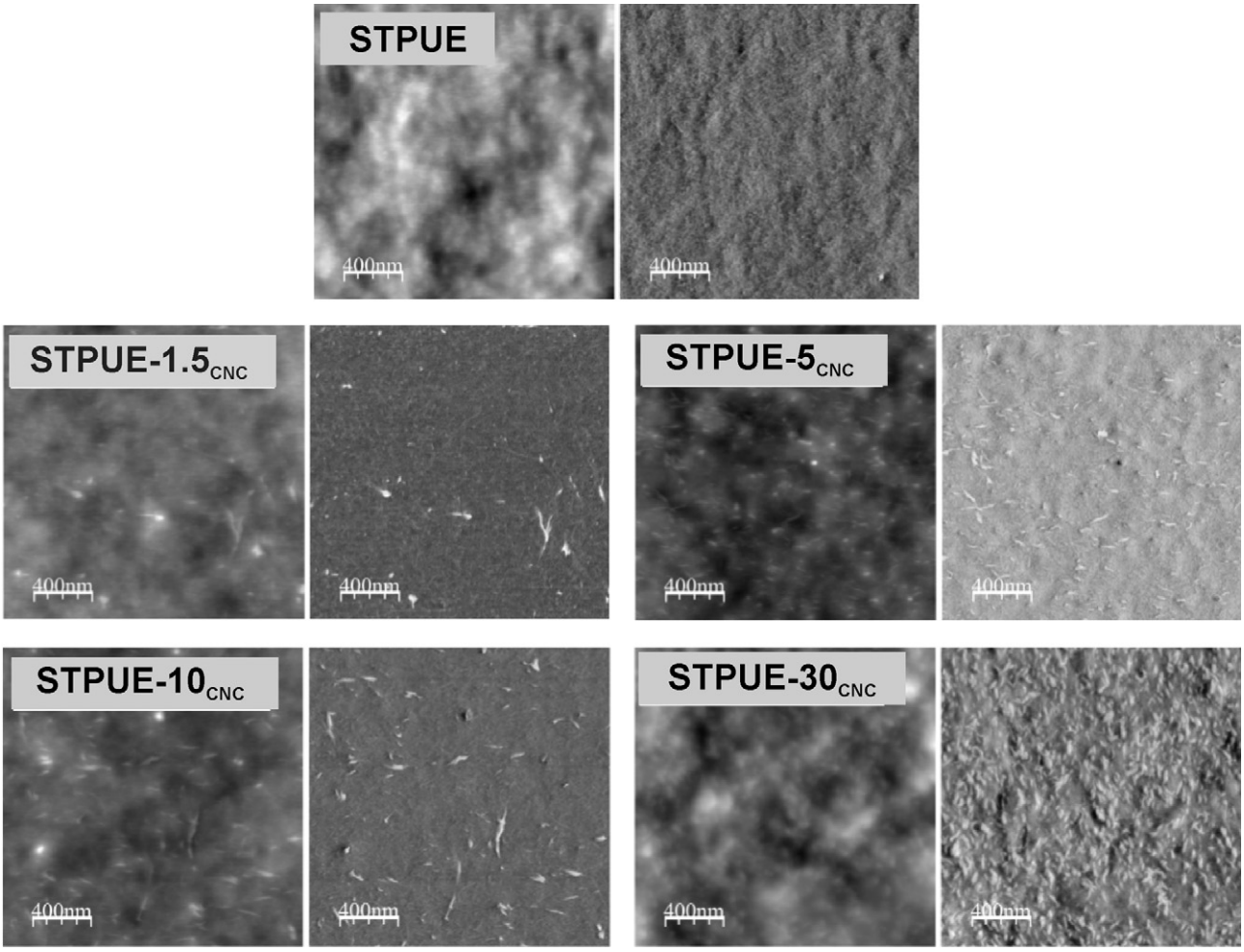

Fig. 5. AFM height (left) and phase (right) images of cryo-ultramicotomed polyurethane and nanocomposites sections.

and is followed by two plastic deformation regions. The region of moderate slope is indicative of soft domain deformation plus rotation and alignment of the smaller hard microdomains. The last region corresponds to the stretching and strain-induced soft segment crystallization as well as further break-up of the hard microdomains (Yeh, Hsiao, Sauer, Michel, & Siesler, 2003) Incorporation of cellulosic nanocrystals resulted in an improvement of both the elastic modulus and yield strength at 50%. However, the elongation at break drastically decreased upon nanocrystals content except for STPUE-1.5$_{CNC}$. As mentioned above, CNC addition resulted in an increase of hard segment crystallization phenomenon and caused ductility loss due to collapse of the jammed structure thus exceeding the stress that can be supported by the soft domains without significant reorientation and alignment, yet did not hinder the interconnected HS network at low strains. In this way, in spite of this increase in E and σ_{50}, it can be observed that STPUE-5$_{CNC}$, STPUE-10$_{CNC}$ and STPUE-30$_{CNC}$ showed an important decrease in ductility avoiding the extension of the soft segment as a consequence of the high CNC content which avoided the SS chains deformation.

5. Conclusions

Cellulose nanocrystals, with an aspect ratio of 17, were successfully extracted from MCC to the incorporation in elastomeric matrices. CNC were used for processing nanocomposites at different contents by a casting/evaporation method using STPUE as matrix. Thermal, mechanical and morphological properties indicated, in general, favorable matrix–nanocrystals interactions arising from efficient dispersion of CNC in polyurethane.

Low CNC quantity in polyurethane nanocomposites leads to a tough material without loss in ductility whereas an increase in CNC content, enhanced the soft and hard segment crystallization, which provoked an increase in the material stiffness and stability versus temperature. It is worth noting that CNC network formation can be directly affected with the polyurethane microstructure and also, with the interactions between SS and HS matrix–nanoreinforcement, mainly due to the high number of hydroxyl groups at CNC surface, which induced crystallization from CNC.

Acknowledgements

The authors wish to express their gratitude to the University of the Basque Country for funding this work (PIFA/01/2006/045) to the Basque Government '*Saiotek 2010*' (S-PE10UN22) and '*Grupos de Investigación Consolidados*' (IT-365-07). We would like to acknowledge General Research Services from the University of the Basque Country (SGIker) for their technical support. This paper is dedicated In memoriam of Dr. Iñaki Mondragon Egaña.

References

Auad, M. L., Contos, V. S., Nutt, S., Aranguren, M. I., & Marcovich, N. E. (2008). Characterization of nanocellulose-reinforced shape memory polyurethanes. *Polymer International*, *57*, 651–659.

Azizi Samir, M. A. S., Alloin, F., & Dufresne, A. (2005). Review of recent research into cellulosic whiskers, their properties and their application in nanocomposite field. *Biomacromolecules*, *6*, 612–626.

Azizi Samir, M. A. S., Alloin, F., Sanchez, J.-Y., El Kissi, N., & Dufresne, A. (2004). Preparation of cellulose whiskers reinforced nanocomposites from an organic medium suspension. *Macromolecules*, *37*, 1386–1393.

Beck-Candanedo, S., Roman, M., & Gray, D. G. (2005). Effect of reaction conditions on the properties and behavior of wood cellulose nanocrystal suspensions. *Biomacromolecules*, *6*, 1048–1054.

Berglund, L. A. (2005). In A. K. Mohanty, M. Misra, & L. T. Drzal (Eds.), *Natural fibers, biopolymers, and biocomposites* (pp. 807–832). Boca Raton, Fla, USA: CRC Press.

Bondeson, D., Mathew, A., & Oksman, K. (2006). Optimization of the isolation of nanocrystals from microcrystalline cellulose by acid hydrolysis. *Cellulose*, *13*, 171–180.

Cao, X., Habibi, Y., & Lucia, L. A. (2009). One-pot polymerization, surface grafting, and processing of waterborne polyurethane–cellulose nanocrystal nanocomposites. *Journal of Materials Chemistry*, *19*, 7137–7145.

Capadona, J. R., Shanmuganathan, K., Trittschuh, S., Seidel, S., Rowan, S. J., & Weder, C. (2009). Polymer nanocomposites with nanowhiskers isolated from microcrystalline cellulose. *Biomacromolecules*, *10*, 712–716.

Chazeau, L., Paillet, M., & Cavaille, J.-V. (1999). Plasticized PVC reinforced with cellulose whiskers. I. Linear viscoelastic behavior analyzed through the quasi-point defect theory. *Journal of Polymer Science Part B: Polymer Physics*, *37*, 2151–2164.

Chen, T. K., Shieh, T. S., & Chui, J. Y. (1998). Studies on the first DSC endotherm of polyurethane hard segment based on 4,4′-diphenylmethane diisocyanate and 1,4-butanediol. *Macromolecules*, *31*, 1312–1320.

Cuve, L., Pascault, J. P., Boiteux, G., & Seytre, G. (1991). Synthesis and properties of polyurethanes based on polyolefine: 1. Rigid polyurethanes and amorphous segmented polyurethanes prepared in polar solvents under homogeneous conditions. *Polymer*, *32*, 343–352.

Dong, X. M., Revol, J.-F., & Gray, D. G. (1998). Effect of microcrystallite preparation conditions on the formation of colloid crystals of cellulose. *Cellulose*, *5*, 19–32.

Dufresne, A. (2000). Dynamic mechanical analysis of the interphase in bacterial polyester/cellulose whiskers natural composites. *Composite Interfaces*, *7*, 53–67.

Eceiza, A., Martin, M. D., de la Caba, K., Kortaberria, G., Gabilondo, N., Corcuera, M. A., et al. (2008). Thermoplastic polyurethane elastomers based on polycarbonate diols with different soft segment molecular weight and chemical structure: Mechanical and thermal properties. *Polymer Engineering and Science*, *48*, 297–306.

Goetz, L., Mathew, A., Oksman, K., Gatenholm, P., & Ragauskas, A. J. (2009). A novel composite film prepared from crosslinked cellulosic whiskers. *Carbohydrate Polymers*, *75*, 85–89.

Golapan Nai, K., & Dufresne, A. (2003). Crab shell chitin whisker reinforced natural rubber nanocomposites 1. Processing and swelling behavior. *Biomacromolecules*, *4*, 657–665.

Habibi, Y., Lucía, L. A., & Rojas, O. J. (2010). Cellulose nanocrystals: Chemistry self-assembly and applications. *Chemical Reviews*, *110*, 3479–3500.

Hajji, P., Cavaillé, J.-Y., Favier, V., Gauthier, C., & Virgier, G. (1996). Tensile behavior of nanocomposites from latex and cellulose whiskers. *Polymer Composites*, *17*, 612–619.

Holt, B. L., Stoyanov, S. D., Pelan, E., & Paunov, V. N. (2010). Novel anisotropic materials from functionalised colloidal cellulose and cellulose derivatives. *Journal of Materials Chemistry*, *20*, 10058–10070.

Horcas, I., Fernández, R., Gomez, Rodriguez, J. M., Colchero, J., Gomez-Herrero, J., et al. (2007). WSXM: A software for scanning probe microscopy and a tool for nanotechnology. *Review of Scientific Instruments*, *78*, 013705–013708.

Hung, H. S., & Hsu, S. H. (2009). The response of endothelial cells to polymer surface composed of nanometric micelles. *New Biotechnology*, *25*, 235–324.

Koberstein, J. T., Galambos, A. F., & Leung, L. M. (1992). Compression-molded polyurethane block copolymers. 1. Microdomain morphology and thermomechanical properties. *Macromolecules*, *25*, 6195–6204.

Liff, S. M., Kumar, N., & Mckinley, G. H. (2007). High-performance elastomeric nanocomposites via solvent-exchange processing. *Nature Materials*, *6*, 76–83.

Ling, N., Huang, J., Chang, P. R., Anderson, D. P., & Yu, J. (2011). Preparation, modification, and application of starch nanocrystals in nanomaterials: A review. *Journal of Nanomaterials*, *2011*, 1–13.

Morin, A., & Dufresne, A. (2002). Nanocomposites of chitin whiskers from *Riftia* tubes and poly(caprolactone). *Macromolecules*, *35*, 2190–2199.

Pei, A., Malho, J.-M., Ruokolainen, J., Zhou, Q., & Berglund, L. A. (2011). Strong nanocomposite reinforcement effects in polyurethane elastomer with low volume fraction of cellulose nanocrystals. *Macromolecules*, *44*, 4422–4427.

Qi, H., Cai, J., Zhang, L., & Kuga, S. (2009). Properties of films composed of cellulose nanowhiskers and a cellulose matrix regenerated from alkali/urea solution. *Biomacromolecules*, *10*, 1597–1602.

Roman, M., & Winter, W. T. (2004). Effect of sulfate groups from sulfuric acid hydrolysis on the thermal degradation behavior of bacterial cellulose. *Biomacromolecules*, *5*, 1671–1677.

Rueda, L., Fernández d'Arlas, B., Zhou, Q., Berglund, L. A., Corcuera, M. A., Mondragon, I., et al. (2011). *Composites Science and Technology*, *71*, 1953–1960.

Rueda-Larraz, L., Fernandez d'Arlas, B., Tercjak, A., Ribes, A., Mondragon, I., & Eceiza, A. (2009). Synthesis and microstructure–mechanical property relationships of segmented polyurethanes based on a PCL–PTHF–PCL block copolymer as soft segment. *European Polymer Journal*, *45*, 2096–2109.

Saiani, A., Novak, A., Rodier, L., Eeckhaut, G., Leenslag, J. W., & Higgins, J. S. (2007). Origin of multiple melting endotherms in a high hard block content polyurethane: Effect of annealing temperature. *Macromolecules*, *40*, 7252–7262.

Schauerte, K., & Sundermann, R. (1994). In G. Oertel (Ed.), *Polyurethane handbook* (p. 41). Munich/Vienna, New York: Hanser Publishers.

Seydibeyoglu, M. O., & Oksman, K. (2008). Novel nanocomposites based on polyurethane and micro fibrillated cellulose. *Composites Science and Technology*, *68*, 908–914.

Shanmuganathan, K., Capadona, J. R., Rowan, S. J., & Weder, Ch. (2010). Bio-inspired mechanically-adaptive nanocomposites derived from cotton cellulose whiskers. *Journal of Materials Chemistry*, *20*, 180–186.

Siqueira, G., Bras, J., & Dufresne, A. (2009). Cellulose whiskers versus microfibrils: Influence of the nature of the nanoparticle and its surface functionalization on the thermal and mechanical properties of nanocomposites. *Biomacromolecules*, *10*, 425–432.

Tien, Y. I., & Wei, K. H. (2006). High-tensile-property layered silicates/polyurethane nanocomposites by using reactive silicates as pseudo chain extenders. *Macromolecules*, *39*, 6133–6141.

Van den Berg, O., Capadona, J. R., & Weder, C. (2007). Preparation of homogeneous dispersions of tunicate cellulose whiskers in organic solvents. *Biomacromolecules*, *8*, 1353–1357.

Wang, C. B., & Cooper, S. L. (1983). Morphology and properties of segmented polyether polyurethaneureas. *Macromolecules*, *16*, 775–786.

Wu, Q., Henriksson, M., Liu, X., & Berglund, L. A. (2007). A high strength nanocomposite based on microcrystalline cellulose and polyurethane. *Biomacromolecules*, *8*, 3687–3692.

Yeh, F., Hsiao, B. S., Sauer, B. B., Michel, S., & Siesler, H. W. (2003). In situ studies of structure development during deformation of a segmented poly(urethane–urea) elastomer. *Macromolecules*, *36*, 1940–1956.